Journal of Molecular Structure, 145 (1986) 45—68
Elsevier Science Publishers B.V., Amsterdam — Printed in The Netherlands

MOLECULAR STRUCTURE AND CONFORMATIONAL EQUILIBRIUM OF GASEOUS THIOPHENE-2-ALDEHYDE AS STUDIED BY ELECTRON DIFFRACTION AND MICROWAVE, INFRARED, RAMAN AND MATRIX ISOLATION SPECTROSCOPY

G. O. BRAATHEN, K. KVESETH and C. J. NIELSEN
Department of Chemistry, University of Oslo, 0315 Oslo 3 (Norway)
K. HAGEN
Department of Chemistry, AVH, University of Trondheim, N-7000 Trondheim (Norway)
(Received 14 November 1985)

ABSTRACT

Thiophene-2-aldehyde has been investigated by microwave, IR and Raman spectroscopy and by electron diffraction of the vapour. The compound was also isolated in argon and nitrogen matrices and studied by IR spectroscopy. Two conformers were identified, a more stable planar isomer with the S atom *syn* to the O atom and a less stable planar (or near planar) *anti* form. Assuming that the geometry of the two forms differs only in the S—C—C=O torsion angle and, assuming the thiophene ring to have C_{2v} symmetry, the electron diffraction study gives the following result for some of the distances (r_a) and angles ($\angle_\alpha$): r(C—H) = 1.114(20) Å, r(C=O) = 1.224(7) Å, r(C—S) = 1.717(4) Å, r(C=C) = 1.375(7) Å, r(C—C) (in the ring) = 1.431(15) Å, r(C—COH) = 1.466(16) Å, ∠C=C—COH = 126.4(1.3)°, ∠C=C—S = 111.8(4)°, ∠C=C—H = 129.2(4.0)°, ∠C—C=O = 123.7(9)°, and ∠ϕ (S—C—C=O torsion angle in the *anti* conformer) = 158.5 (23.1)° At 94°C the observed amount of the conformer with O and S *syn* was 80.5(7.9)%, and the *syn* conformer had a r.m.s. torsional amplitude of vibration of τ = 17.2(13.6)°. Assuming $\Delta S^\circ = 0$, the obtained amount of *syn* corresponds to ΔH° = 4.3 ± 1.6 kJ mol^{-1}. The matrix isolation study included the use of a heatable nozzle, which made it possible to trap different conformational equilibria in the matrices. By comparing absorbances obtained for different temperatures, the enthalpy difference between the conformers was estimated as 4.1 ± 0.4 kJ mol^{-1}, in very good agreement with the electron diffraction result. The matrix data support the extensive IR and Raman study of the other phases (vapour, liquid, solution and solid). In the crystalline solid the preferred conformation was found to be *syn*. The microwave investigation shows the planarity of the *syn* isomer, whereas the *anti* form was not detected. The spectral data have hence been interpreted in terms of C_s symmetry, and a normal coordinate analysis has been carried out for both conformers. The final structural refinement was based upon electron diffraction intensities in combination with the microwave rotational constants. The vibrational amplitude parameters applied were derived from the force field calculations.

0022-2860/86/$03.50

INTRODUCTION

The conformation of 2-substituted furan and thiophene carbonyl compounds has been the subject of a large number of investigations. For furan-2-aldehyde it has been shown that in solution the conformational equilibrium between the two forms with C=O and C—O bonds *anti* or *syn* depends on the solvent used [1, 2]. An electron diffraction investigation showed that in the gas phase 69 ± 9% of the furan-2-aldehyde molecules had the two bonds *anti* to each other [3]. For the corresponding acid chloride, 2-furoyl chloride, a gas phase electron diffraction experiment [4] found the conformers with C=O and C—O *syn* to be the most abundant form with 70 ± 14% present at 86°C.

In an early microwave spectroscopy investigation of thiophene-2-aldehyde (hereafter called TA) only one conformer was observed [5], and it was assumed to be the O—S *anti* isomer (see Fig. 1 for a description of the possible conformers). However, a comparison between the observed moments of inertia [5] and values calculated for models of the two rotamers indicated that the observed spectrum rather corresponds to the O—S *syn* form [6]. Ultrasonic relaxation in the pure liquid [7] gave an energy difference between the conformers of less than 6.7 kJ mol^{-1}. This experiment could not determine if *syn* or *anti* was the low-energy form. From measurements of dipole moments and molar Kerr constants [8], it was concluded that TA in cyclohexane solution had 83 ± 10% of the molecules in the *syn* conformation. Only this *syn* form had been detected in the ^{1}H NMR studies [9—12], while the occurence of an equilibrium between rotatonal isomers have been established by ^{13}C NMR spectroscopy [13]. Kao and Radom [14] used ab initio molecular orbital calculations to study the molecular structure and conformation of TA and found an energy difference of 3.0—3.6 kJ mol^{-1} between the two conformers.

Gas phase electron diffraction offers another possibility of studying the conformation of TA, and in addition, this method can also determine bond distances and valence angles. Infrared and Raman spectroscopy is also well suited to detect the existence of conformational mixtures, and the isolation in a low temperature inert gas matrix of a thermal molecular

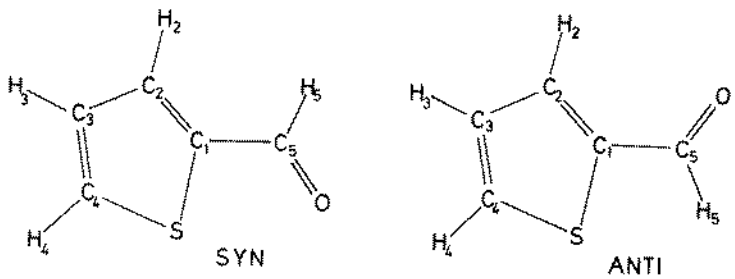

Fig. 1. Diagrams of conformers of thiophene-2-aldehyde.

beam [15] has proved to be a valuable tool in the elucidation of conformational problems. Moreover, spectroscopic data support the electron diffraction analysis. With as much as ca. 15% of the less stable conformer present at room temperature we also hoped that a microwave investigation could give added information. We therefore decided to make a combined spectroscopic and electron diffraction study of thiophene-2-aldehyde, and the results are reported herein.

EXPERIMENTAL

Sample

TA was kindly given to us by S. Gronowitz, University of Lund (Sweden), and further purified by destillation in vacuo. The purity, checked by gas chromatography, was better than 99.7%, and none of the recorded microwave, IR and Raman spectra indicated the presence of impurities.

Microwave spectroscopy

Microwave spectra were recorded at ca. 10 mTorr at room temperature and at −40°C in the region 12.5—40 GHz using a Hewlett Packard 8460A MRR spectrometer. Stark voltages in the range 100—1800 V cm^{-1} were applied.

Infrared and Raman spectroscopy

Infrared spectra in the region 5000—200 cm^{-1} were recorded on Perkin Elmer models 125 and 225 spectrometers. Vapour spectra in this region were recorded at ambient temperatures in 10 cm, 1 m and 10 m cells equipped with windows of KBr, KRS-5 and CsI, respectively. The liquid was studied in various sealed cells of different thickness and window materials, and solution spectra were recorded in non-polar (CS_2, CCl_4) as wells as in highly polar (DMSO, CH_3CN) solvents. Low temperature spectra of the unannealed and annealed solid were recorded at ca. 77 K.

TA mixed with argon or nitrogen was condensed on the cold CsI window of an Air Products Displex cryostat at a rate of ca. 5 mmol h^{-1}. The temperature of the window was ca. 18 K during the deposition and ca. 12 K during the recording of the spectra. The M/A ratios were ca. 1200 and 1500 for the argon and nitrogen matrices, respectively. These values were obtained by standard manometric techniques. Prior to the deposition on the cold window the sample/matrix gas mixture was led through a quartz nozzle surrounded by a heating wire. The argon matrix experiments were performed at three different temperatures; 313 K(ambient), 585 K and 827 K, whereas the nitrogen matrix experiments were performed at two different temperatures; 313 K and 895 K. The temperature was measured with a thermocouple

situated in the nozzle opening and was verified by measuring the temperature effect on the conformational equilibrium of 1,2-dichloroethane, for which ΔH° is already known [16—20]. The matrices were annealed at 37 K (Ar) and 34 K (N_2). The temperature was measured with a thermocouple placed near the cold window and was calibrated against the $\alpha \rightarrow \beta$ phase transition of solid nitrogen at 35.6 K.

The far IR spectra (400—20 cm^{-1}) were studied at ambient temperature using a RIIC Fourier spectrometer model 520, equipped with a light pipe gas cell [21] with a 6 m optical path length. The far IR spectra of the neat liquid were recorded on a Perkin-Elmer/Hitachi grating spectrometer, model FIS-3, while the solution spectra were recorded with a Bruker model 114C FT spectrometer.

Raman spectra were obtained on a modified [22] Cary 81 Raman spectrometer using the 514.5 and 488.0 nm lines of an Ar^+ laser for excitation. The liquid sample was studied in a sealed glass tube and semiquantitative polarization data were obtained. Low temperature (77 K) spectra of the sample deposited on a copper block were obtained from both the amorphous and the polycrystalline solids.

Electron diffraction studies

Diffraction photographs were made with the Balzers Eldigraph KDG-2 [23, 24] at the University of Oslo on Kodak Electron Image plates with a nozzle-tip temperature of 367 K. Five plates from each of the two nozzle-to-plate distances (250.12 and 500.12 mm) were selected for analysis. The electron wavelength was calibrated against benzene [25]. The procedures for obtaining the total scattered intensity distribution, $s^4I_t(s)$, and the molecular intensity, $sI_m(s)$, have been described previously [26—28]. Data

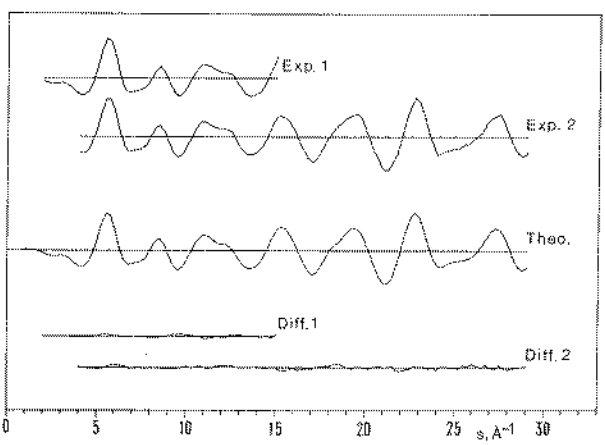

Fig. 2. Intensity curves, $sI_m(s)$. Experimental curves are averages of all plates for the two camera distances. The theoretical curve was calculated from the parameters in Table 6.

from the long and short camera distances were obtained over the ranges $2.00 \leqslant s \leqslant 15.00$ and $5.00 \leqslant s \leqslant 29.50$ Å^{-1}, respectively, at intervals of $\Delta s = 0.25$ Å^{-1}. The average experimental intensity curves are shown in Fig. 2; the individual curves and backgrounds are available as supplementary material [29].

RESULTS

Microwave investigation

The microwave spectrum of TA has previously been studied by Mönnig et al. [5], who only found one conformer present in the vapour phase. The dipole moment was determined to be: $\mu_a = 3.00$ D, $\mu_b = 1.84$ D. Hence, the spectrum, although dominated by intense μ_a R-type transitions, is very rich in lines. Further, a large number of lines due to vibrationally excited states are present in the spectrum, complicating the search for other conformers.

From the reported rotational constants [5], based upon a small number of low-J transitions, the complete vibrational ground state rotational spectrum was calculated. Then, within 5—100 MHz of their precalculated positions the strongest high-J transitions were identified and measured. A revised set of rotational and distortion constants then allowed the weaker transitions to be identified and measured. This procedure was repeated until the entire rotational spectrum of the vibrational ground state could be predicted within ca. 0.05 MHz. The number and types of the measured transitions are summarized in Table 1*. Table 2 summarizes the final analysis in terms of the Watson [30] rotational and distortion constants.

TABLE 1

Number and type of observed rotational transitions for the vibrational ground state[a]

	R-type		Q-type		MWPROG r.m.s.[b] (MHz)
	μ_a	μ_b	μ_a	μ_b	
N_{obs}	75	11	3	46	0.0195
J_{max}	14	14	50	37	

[a] J_{max} = maximum rotational quantum number; R, Q, μ_a and μ_b in conventional sense. [b] Modified FORTRAN version of ROTFIT originally written by G. O. Sørensen, H. C. Ørsted Institute, University of Copenhagen.

*The microwave spectrum of TA is available from the authors upon request, or from the Microwave Data Center, Molecular Spectroscopy Section, National Bureau of Standards, Washington, D.C. 20234, U.S.A., where they have been deposited.

TABLE 2

Rotational parameters[a] for the vibrational ground state and vibrational excited states of thiophene-2-aldehyde

	Ground state	$v_{27} = 1$ ($\nu_{27} = 122$ cm^{-1})	$v_{19} = 1$ ($\nu_{19} = 173$ cm^{-1})	$v_{26} = 1$ ($\nu_{26} = 257$ cm^{-1})
A	5113.0010 (12)	5078.59 (8)	5142.5 (3)	5113.06 (23)
B	1887.85455 (22)	1887.090 (4)	1890.254 (8)	1887.107 (6)
C	1378.74107 (19)	1380.409 (4)	1378.265 (8)	1379.208 (4)
Δ_J	0.1477 (8)	0.139 (13)	—[b]	—
Δ_{JK}	0.854 (4)	0.745 (16)	0.89 (5)	0.889 (28)
Δ_K	0.246 (23)	—	—	—
δ_J	0.03962 (17)	—	—	—
δ_K	0.678 (5)	—	—	—
ID	0.00893 (5)	−1.2122 (24)	1.043 (8)	−0.220 (6)

[a]Rotational constants (A, B, C) are in units of MHz, Watson distortion constants (Δ, δ) are in units of kHz and inertial defects (ID) in units of u Å^2. Numbers in parentheses represent one standard error. [b]Fixed on ground state value.

Of the large number of lines due to vibrationally excited states, the three strongest satellites, corresponding to $v_{27} = 1$, $v_{19} = 1$ and $v_{26} = 1$ and identified by their relative intensity and inertial defect, were measured. The rotational parameters for these states are included in Table 2. The rotational spectrum of at least five other excited states can easily be measured. However, this remains for future work.

The most probable conformations of TA are the planar OS *syn* and OS *anti* forms. In order to settle which one of these is responsible for the observed spectrum a substitution-type structure was evaluated. By using the difference between the observed moments of inertia and those of thiophene [31], stripped of one α-hydrogen atom, it is possible to calculate two structural parameters for the aldehyde group. Assuming the r_s structure of the aldehyde group to be equal to that in acrolein [32], the C—C_{ald} distance and the C=C—C_{ald} angle can be estimated. For the O—S *syn* form this procedure gave: r(C—C) = 1.44 Å and ∠C=C—CHO = 122°, whereas the results for the OS *anti* form were r(C—C) = 1.36 Å and ∠C=C—CHO = 136°. The last result is clearly unacceptable, and it must be concluded that the *syn* form is dominating in the vapour phase.

Analysis of the vibrational spectra

The vibrational spectra of TA have been recorded and analysed by several authors [33—40]. Comparisons between the spectra of different substituted thiophenes [37] and extensive investigations of the carbonyl stretching region [39, 40] have led to a good understanding of the vibrational spectrum. However, no complete analysis has heretofore been published.

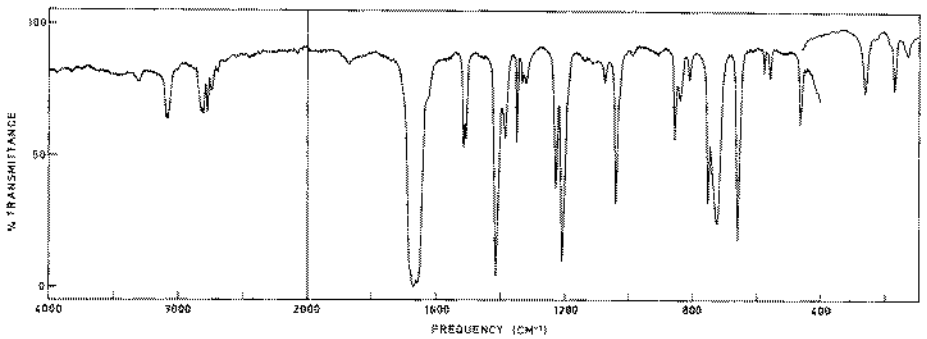

Fig. 3. IR spectrum of liquid thiophene-2-aldehyde.

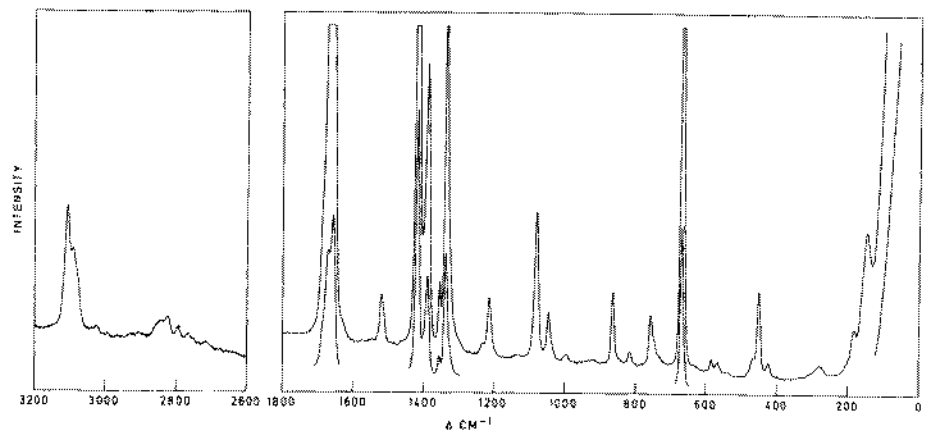

Fig. 4. Raman spectrum of thiophene-2-aldehyde in the liquid phase.

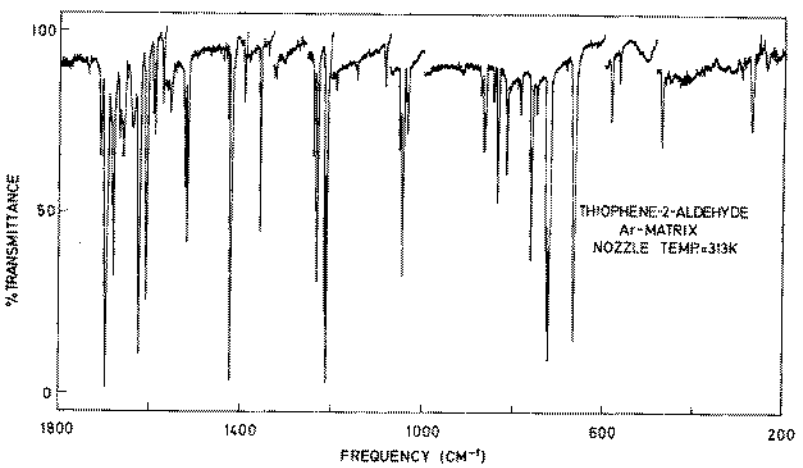

Fig. 5. IR spectrum of thiophene-2-aldehyde isolated in argon. M/A = 1200. Nozzle temperature = 313 K (ambient).

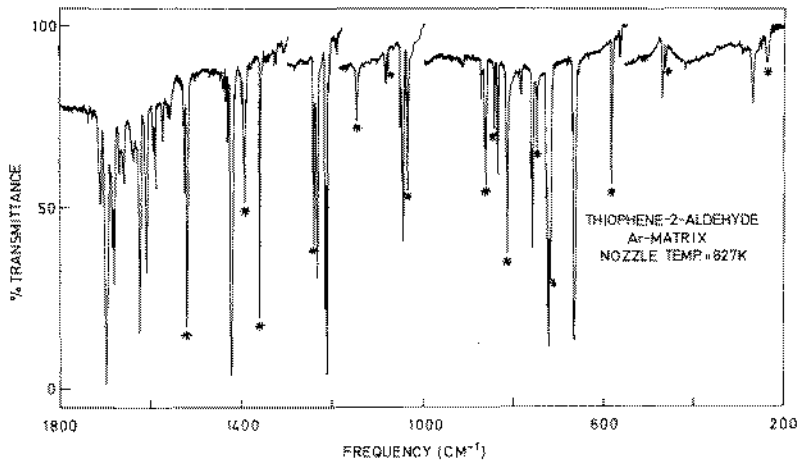

Fig. 6. IR spectrum of thiophene-2-aldehyde isolated in argon. M/A = 1200. Nozzle temperature = 827 K. Bands marked with an asterisk belong to the less stable *anti* conformer.

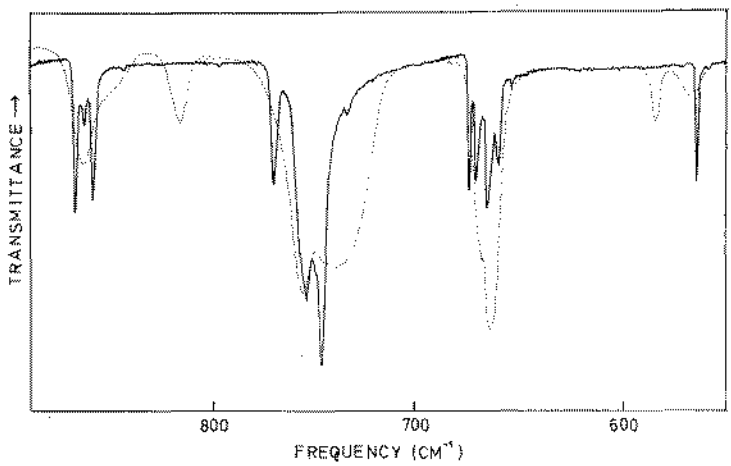

Fig. 7. IR spectrum of solid thiophene-2-aldehyde at T = 90 K; dotted line, amorphous solid (unannealed); solid line, crystalline solid (after annealing).

Infrared and Raman spectra of the neat liquid are shown in Figs. 3 and 4, respectively. Figs. 5 and 6 show the mid IR spectra (1750—200 cm^{-1}) of TA isolated in argon using a nozzle temperature of 313 K (ambient) and 827 K, respectively. Finally, the effect of annealing the amorphous solid is shown (900—500 cm^{-1}) in Fig. 7. The wavenumbers of the observed bands are listed in Table 3. Matrix data refer to the argon matrix experiments, but some bands which obviously are due to matrix effects, as seen by comparison with the nitrogen matrix spectra, have been omitted.

As seen from Table 3 and Fig. 7, a number of IR and Raman bands present in the liquid spectra vanished in the crystalline spectra. They are marked

TABLE 3

Infrared and Raman spectral data[a] for thiophene-2-aldehyde

Infrared				Raman		Assignments
Vapour	Matrix	Liquid	Cryst.[b]	Liquid	Cryst.	
3398 w,A/B[3]		3320 w	3292 w			$2\nu_5$
		3180 vw	3210 w,bd			$\nu_3 + \nu_{27}$
3126, 3115, 3104 vw,B	3122 vw	3107 m	3098 s	3105 m,P	3099 s	ν_1 (*syn*)
3099 vw,A		3091 m	3092 s	3089 m,P	3092 m	ν_2 (*syn*)
3093, 3086, 3081 vw,A			3076 m		3076 m	ν_3 (*syn*)
			3032 vw			$2\nu_6$
		3022 vw	3026 vw	3020 vw,P	3027 w	$\nu_5 + \nu_9$
		2925 vw	2926 vw			$\nu_6 + \nu_7$
		2900 vw	2899 vw	2903 vw	2901 vw	$\nu_5 + \nu_{11}$
			2887 vw			$\nu_6 + \nu_8$
			2866 vw			
2843, 2832 w,sh,B	2838 m	2838 m,bd		2840 w,bd,P		$\nu_6 + \nu_9$ FR
2826, 2815 s,B	2828 m	2821 m	2826 m,bd	2822 w,P	2827 m	ν_5 (*syn*) FR
			2819 m		2821 m	$2\nu_7$ FR
2801, 2796, 2790 s,A	2796 m	2791 m	2788 m,bd	2792 w,P	2790 w	$\nu_7 + \nu_8$ FR
2763, 2758, 2753 m,A		2763 w	2756 m	2763 vw,P	2756 vw	$\nu_5 + \nu_{12}$
2745, 2731 w,B		2750 w	2748 w,sh			$\nu_7 + \nu_9$
2716, 2711, 2705 w,A		2712 vw		2714 vw,P	2711 vw	$\nu_6 + \nu_{11}$
		1895 vw,sh	1896 vw, 1889 vw, 1881 vw			Comb.[c]
1868 w,A/B		1877 w,bd		1876 vw		Comb.
			1846 vw,bd			Comb.
		1830 vw,bd	1834 vw			Comb.
		1755 vw,sh	1774 vw			Comb.
		1745 w,sh				Comb.
			1694 w		1694 w	$\nu_{14} + \nu_{22}$
1711, 1705, 1698 vs,A	1698, 1696 vs	1688 s,sh	1672 m	1687 m,sh	1674 m	ν_5 (*syn*) FR
1676 w,sh	1683, 1678 ms	1675 vs	1664 m	1672 vs,P		Comb. FR
		1661 s,sh	1654 m	1656 vs,P	1658 s	Comb. FR
			1650 s	1633 m	1648 vs	Comb. FR
			1625 vw			$\nu_{21} + \nu_{23}$
			1616 w		1618 w	$\nu_{13} + \nu_{24}$
			1554 w			Comb.
1531, 1527, 1520, 1516 m,?	1524 m	1520 m	1522 m	1519 m,P	1522 m	ν_6 (*syn*)
	1519 ms†	1514 m	*	1513 w,sh	*	ν_6 (*anti*)
		1506 w,sh				Comb.
			1497 vw			Comb.
			1461 vw			Comb.
		1440 vw				Comb.

TABLE 3 (continued)

Infrared				Raman		Assignments
Vapour	Matrix	Liquid	Cryst.[b]	Liquid	Cryst.	
1430 1424 s,A 1418	1429 w 1422 vs	1420 s	1419 s,bd	1419 vs,P	1424 s 1419 s	ν_7 (*syn*)
1395 w,sh,B?	1393 w↑	1390 m	*	1390 s,P	*	ν_8 (*anti*)
	1380 vw		1380 vw		1380 m	ν_8 (*syn*)
			1372 vw			Comb.
1366 1360 m,A 1353	1358 ms↑	1355 m	*	1356 m,P	*	ν_9 (*anti*)
	1340 vw	1338 w	1338 w 1333 w	1340 vs,P	1340 s	ν_9 (*syn*)
1334						Comb.
1328 vw,A	1328 vw↑					
1322	1324 vw	1325 w	1325 m	1327 m,sh	1326 m,sh	Comb.
			1314 vw,sh			Comb.
1247 1242 m,A 1238	1241 m↑					ν_{10} (*anti*)
1234 m,A 1228	1232 ms	1235 m	1235 s	1235 w,P	1238 w	ν_{10} (*syn*)
1215 1211 s,A 1204	1211 s	1215 s	1216 s	1215 m,P	1218 m	ν_{11} (*syn*)
	1190 w↑		1200 m			Comb.
			1184 vw			Comb.
1151 1145 vw,? 1139	1146 w↑	1146 vw				ν_{11} (*anti*)
			1130 w			
		1116 vw	1123 vw			
1087 1078 w,B	1084 w 1079 vw↑	1080 w	1086 m	1082s,P	1090 m	ν_{12} (*syn*) ν_{12} (*anti*)
1052 1047 m,A 1040	1044 s	1046 m	1052 w,sh 1047 s	1048 m,P	1049 m	ν_{13} (*syn*)
			1039 vw			
1031 w,sh?	1034 m↑	1035 w,sh		1036 w,sh	*	ν_{13} (*anti*)
			1032 vw			Comb.
	990 vw	995 vw	990 w	994 w,D	990 w	ν_{20} (*syn*)
		940 vw				
	911 vw	917 vw,bd	923 m	920 w,D	926 w	ν_{21} (*syn*)
870 860 m,B	864 mw	864 m	868 m 864 w 860 m	866 m,P	867 m	ν_{14} (*syn*)
	862 mw↑					ν_{14} (*anti*)
844 w,?	844 w↑					ν_{22} (*anti*)
834 m,C	834 m	846 m,bd	845 vw			ν_{22} (*syn*)
821 815 m,A 810	815 m↑	817 m	*	816 w,P	*	ν_{15} (*anti*)
	785 w		797 vw			$\nu_{17} + \nu_{27}$
767 762 m,A 755	760 ms	757 m	770 m 755 s,bd	758 m,P?	765 w,sh 758 m	ν_{15} (*syn*)
	749 w↑	746 w,sh	*	748 w,sh	*	ν_{16} (*anti*)
727 720 716 s,C 711 710	727 724 s 721 718 ms↑	728 s,bd	747 s 735 vw	729 vw,sh	749 w,sh	ν_{23} (*syn*) ν_{23} (*anti*)
		669 m,sh	675 m 672 s	672 vs,P	674 s	ν_{16} (*syn*)

TABLE 3 (continued)

Infrared				Raman		Assignments
Vapour	Matrix	Liquid	Cryst.[b]	Liquid	Cryst.	
671 665 659 s,A	665 s	664 s	666 s 661 m,sh	663 w,sh	667 w,sh	ν_{17} (*syn*)
			654 w			$\nu_{19} + \nu_{25}$
582 vw,A	583 m↑	584 w	*	583 w,P	*	ν_{17} (*anti*)
			572 vw			
573 565 556 vw,C	566 mw	565 w	564 m	568 w	568 w	ν_{24} (*syn*)
			558 vw			
477 469 460 w,C	471 m	469 m	471 m 466 w	472 w	474 w,sh	ν_{25} (*syn*)
	464 vw↑					ν_{24} (*anti*)
	454 vw	452 vvw	456 vw	454 s,P	459 m	ν_{18} (*syn*)
	420 vw↑	424 vw	*	427 w,P	*	ν_{18} (*anti*)
	293 w					
	277 m↑,N_2					
266 257 250 w,C	270 m	274 m	284 s,bd	279 w,bd,D	286 vw	ν_{26} (*syn*)
	238 w↑	240 vw,sh				ν_{26} (*anti*)
			230 vw,bd			
	216 vs,N_2					
		195 vw,sh				ν_{19} (*anti*)?
178 168 w,B		182 m	198 m 191 vw	185 w	197 vw 192 vw	ν_{19} (*syn*)
129 122 114 w,C		145 w	165 w 159 w	150 m,D	169 w,sh 162 m	ν_{27} (*syn*)
			84 w		101 m 85 m 73 ms 51 s 38 w	l.m.

[a]Bands in the region 5000—3400 and 2700—1900 cm^{-1} were omitted. Matrix data refer to the Ar matrix, but some bands which obviously are caused by matrix effects are omitted. [b]Abbreviations: s, strong; m, medium; w, weak; v, very; bd, broad; A, B and C denote vapour band contours; P, polarized; D, depolarized; FR, Fermi resonance; sh, shoulder; ↑, bands gaining intensity upon increased nozzle temperature; asterisks (*) denote bands disappearing in the crystal; Cryst., polycrystalline phase at $T = 90$ K; l.m., lattice modes; N_2, bands observed in nitrogen matrix only. [c]Combination bands; used when more than one binary combination is possible.

with asterisks in Table 3 and are attributed to the second conformer (*anti*), present in the vapour and the liquid but absent in the crystal. Moreover, it can be seen from Table 3 that these bands are either overlapped, absent or relatively weak in the vapour spectrum. We therefore conclude that the conformer present in the crystalline state also dominates in the vapour phase. This assertion is in agreement with the results from our matrix experiments, as explained below.

The IR spectra of TA were further recorded with samples dissolved in polar and non-polar solvents, and relative band intensities were compared

to those in the liquid. We found no marked changes in the relative band intensities and conclude that the total dipole moment of the two conformers are of approximately the same magnitude.

The small halfwidths (full width at half height, FWHH = 0.5—2 cm^{-1}) of the IR absorptions of the matrix isolated sample enabled us to separate bands which overlapped in the other phases (vapour, liquid, solution and solid). Most of the *anti* fundamentals, which were covered by close-lying and more intense *syn* bands in the other phases were resolved in the matrix spectra.

Most of the bands are multiplets, containing two or more components within 10—15 cm^{-1}. This multiplet structure can in some cases be ascribed to multiple trapping sites in the matrix. Upon increased nozzle temperature some multiplet components gained intensity according to van't Hoff's equation, whereas others showed no temperature effect. Absorptions gaining intensity are marked with an asterisk in Fig. 6 and with an arrow (↑) in Table 3. These bands no doubt belong to the less stable *anti* conformer. The components which showed no temperature effect must be attributed to matrix effects like multiple trapping sites.

In addition, most of the bands gaining intensity are present in both matrix media (Ar and N_2) which is not the case for the components ascribed to matrix effects. Moreover, the bands which disappeared upon annealing of the amorphous solid coincide with the bands gaining intensity upon increased nozzle temperature in the matrix spectra. This observation supports the assumption that bands gaining intensity upon increased nozzle temperature belong to the less stable *anti* conformer.

Annealing of the matrices at 37 and 34 K for argon and nitrogen, respectively, led only to minor changes in the spectra, probably due to a rearrangement among different trapping sites. If the barrier separating the two conformers is low enough (less than ca. 12 kJ mol^{-1}), annealing of the matrix can cause the less stable conformer to vanish. In the case of TA, however, the barrier has been measured to be ca. 45 kJ mol^{-1} [7], which means that we cannot expect the interconversion to take place in the temperature interval offered by the Ar and N_2 matrices.

As discussed above, increasing the nozzle temperature leads to an increased concentration of the less stable *anti* conformer. Measuring the absorbance ratio of selected band pairs at different nozzle temperatures makes it possible to calculate ΔH^0 by means of a van't Hoff plot

$$\ln(A_a/A_s) = \text{constant} - \Delta H^0/RT$$

where A_a and A_s are absorbances of *anti* and *syn* bands, respectively, and T is the nozzle temperature. The validity of this procedure for determining ΔH^0 has been shown by comparing the obtained ΔH^0 with values from gas phase studies [16, 41—45]. The selected bandpairs are: 1524/1519 cm^{-1} (Ar), 1232/1393 cm^{-1} (Ar), 1044/1034 cm^{-1} (Ar), 834/815 cm^{-1} (Ar), 760/583 cm^{-1} (Ar), 1525/1037 cm^{-1} (N_2), 1233/817 cm^{-1} (N_2), 760/583 cm^{-1} (N_2).

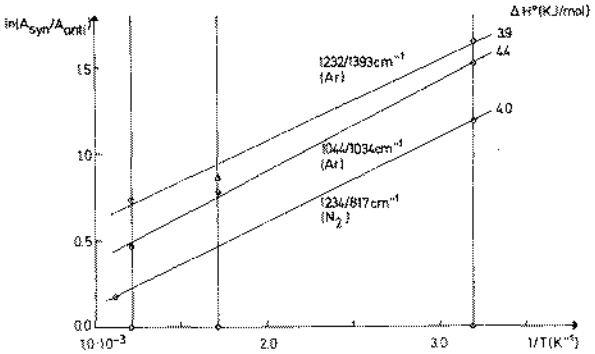

Fig. 8. Van't Hoff plot for three of the band pairs used in the estimation of the enthalpy difference between the two conformers.

The nozzle temperatures were 313 K (Ar and N_2), 585 K (Ar), 827 K (Ar) and 895 K (N_2). All together, 27 absorbance ratios measured for the band pairs at the different temperatures were included in a least squares fitting procedure. The van't Hoff plot for three of these band pairs is depicted in Fig. 8. The calculated value of ΔH° is 4.1 ± 0.4 kJ mol^{-1} (3 σ limit).

The planarity of the most abundant form of TA in the vapour phase (OS *syn*) is well established from the present microwave investigation. Accordingly, the vibrational spectra have been interpreted in terms of C_s symmetry. The 27 fundamental frequencies divide into 19 A' + 8 A'' with all modes being active in both IR and Raman, the A' modes being polarized and having *A/B* hybrid contours and the A'' modes *C*-type contours. From the rotational constants determined by microwave spectroscopy the *PR* separations were calculated [46] to be ca. 12, 9 and 18 cm^{-1} for the *A*, *B* and *C* bands, respectively.

The assignments of the fundamentals above 450 cm^{-1} given by Peron et al. [37] are essentially confirmed by the present work. With the aid of the vapour phase IR band contours and Raman polarization data the assignment is straightforward, and only a few comments will be given here.

Several bands are observed in the C—H_{ald} stretching region. We believe that the band at 2821 cm^{-1} is the fundamental, while the other bands can be explained as overtones or combination bands in Fermi resonance with the fundamental.

The carbonyl stretching region is very complex in the liquid and solid phases, while essentially only one band is observed in the vapour phase spectrum. The complex features in the liquid phase have been thoroughly investigated by Chadwick et al. [39, 40] and by Andrieu et al. [38] and are explained by Fermi resonance.

The C—H_{ald} out-of-plane bending, expected near 1000 cm^{-1}, was assigned to the weak, broad band at 995 cm^{-1}. This band seems depolarized in the Raman spectrum, and in the crystal spectrum it shows up as a single sharp band. Two fundamentals are expected around 650 cm^{-1} due to the C—S

TABLE 4

Suggested valence force constants for thiophene-2-aldehyde[a]

Description	Original value[b]	Final value	Description	Original value[b]	Final value
Stretch			C—S,C=C—H(α); C common		
C—H(α)	5.314	5.314	C=C,S—C—H; C common	—0.115[e]	—0.131[e]
C—H(β)	5.193	5.196	C=C,C—C—H; C common		
C*—H	4.243	4.351	C—C,C=C—H(β)		
C—C*	4.822	5.522	C—S,S—C—C*; C—S common	0.115[e]	0.370[e]
C—C	6.574	6.560	C=C,C=C—C*; C=C common		
C=C	8.704	9.104	C—S,C=C—C*; C common	—0.115[e]	—0.370[e]
C—S	4.794	4.976	C=C,S—C—C*; C common		
C=O	10.772	11.992	C—C,C—C=C		
			C—S,S—C=C; C—S common		
Bend			C=C,S—C=C; C=C common	1.085	1.165
S—C—H C=C—H(α)	0.418	0.419	C=C,C=C—C; C=C common		
			C—S,C—S—C		
C—C—H C=C—H(β)	0.435	0.438	C—C*,S—C—C*; C—C* common	0.545	0.0[c]
			C—C*,C=C—C*; C—C* common		
C—S—C* C=C—C*	0.612	0.484	C=O,O=C—H	0.365	0.556
			C=O,C—C=O	0.0	0.500[c]
S—C=C C—C=C	1.173	1.138	C—C*,C—C*—H	0.0	0.262
			C—C*/C—C=O	0.0	0.285
C—S—C	1.596	1.594			
C—C=O	1.006	1.250	*Bend—bend*		
O=C—H	0.827	0.628	C—C—H,C—C—H		
C—C*—H	0.435		C=C—H(α),C=C—H(β); C=C common	—0.020	—0.0265
			C=C—C*,C=C—H; C=C common		
Out-of-plane bend			C—S—C,S—C—H		
C—H(α)	0.333	0.349	C—S—C,S—C—C*		
C—H(β)	0.400	0.414	S—C=C,C=C—H(β); C=C common	0.040	0.0548
C—C*	0.367	0.484	C—C=C,C=C—H(α); C=C common		
C*—H	0.296	0.384	C—C=C,C=C—C*; C=C common		

Torsion		
$\tau(\alpha\beta)$	1.049	0.942
τ(C—C*)	0.100	0.0535
Stretch—stretch		
C=C,C—C C=C,C—S; C common	0.973	1.195
C—S,C—S	0.215	0.298
C=C,C=C	—0.675	—0.598
C—C,C—S	—0.854	—0.998
C=C,C—S; C not common	—0.500	—0.590
C—S,C—C*; C common	—0.202	0.735
C=C,C—C*; C common	0.237	0.980
C=O,C—C*	0.0	0.976
C=O,C*—H	0.0	0.520[c,d]
Stretch—bend		
C—S,S—C—H; C—S common C=C,C=C—H(α); C=C common C=C,C=C—H(β); C=C common C—C,C—C—H	0.115[e]	0.131[e]
C—C=C,C—C—H; *anti*		
C—C=O,C=C—C* *anti*	0.0	0.180
C—C=O,C=C—C* *syn*	0.0	0.0387
Out-of-plane bend—Out-of-plane bend		
C—H(α),C—C*(α')	0.0430[c]	
CH(β),C—H(β')	—0.0320[c]	
C—H(α),C—H(β) C—C*(α),C—H(β)	—0.0700[c]	
C—H(α),C—H(β') C—C*(α),C—H(β')	0.0130[c]	
Out-of-plane Bend—torsion		
C—H(α),$\tau(\alpha\beta)$ C—C*(α),$\tau(\alpha\beta)$	0.311	0.299
C—H(β),$\tau(\alpha\beta)$	—0.289	—0.294
C—H(α),$\tau(\alpha'\beta')$ C—C*(α),$\tau(\alpha'\beta')$	—0.075[e]	
C—H(β),$\tau(\alpha'\beta')$	—0.073[e]	
C—C*,τ(C—C*)	0.0	—0.0181
Torsion—torsion		
$\tau(\alpha\beta),\tau(\alpha'\beta')$	—0.186	—0.136

[a]Stretch constants are in units of mdyn A^{-1}; stretch—bend interaction constants are in units of mdyn rad^{-1}; bending and torsion constants are in units of mdyn Å rad^{-2}. C* denotes the aldehyde carbon. $\tau(\alpha\beta)$ and τ(C—C*) denote the torsions about the C=C and C—C* bonds, respectively. α and α', likewise β and β', denote α and β positions on opposite sides of the ring. [b]Valence force constants of the thiophene ring from ref. 47 and of the aldehyde group from ref. 48. [c]Constrained during refinement. [d]Estimated, see text. [e]Constrained on opposite sign.

stretching and C—C=O bending modes. The former gives rise to a very strong Raman band in the analog acetyl compound [37]. A doublet at 664 (strong) and 669 (medium) cm^{-1} are observed in the IR spectrum. In the Raman spectrum the intensities are reversed.

Most of the *anti* absorptions are situated close to the corresponding *syn* bands, and the assignments have hence been quite straightforward for most of the fundamentals. In some cases the *anti* bands are situated mid-way between *syn* fundamentals, and the attributions have in these cases been supported by the force constant calculations.

Force constant calculations

An initial valence force field for TA was constructed by transferring force constants from thiophene [47] and ethanal [48]. The molecular geometry was taken as the preliminary r_a-structure, which was not very different from the final one. For the in-plane vibrations a redundant set of internal coordinates was used, whereas the out-of-plane vibrations were calculated using a non-redundant set. The torsion of the aldehyde group was described by the normalized sum of the two *trans* torsions: S—C—C—H_{ald} and C=C—C=O. For the definitions of the ring torsions and out-of-plane bendings, see ref. 47.

The force constants for thiophene [47] were derived by the overlay technique using various isotopes of thiophene and methylated thiophenes. It was considered advantageous to apply the same method for the in-plane vibrations in the present case. For the out-of-plane vibrations, force constants of the thiophene ring were transferred without modifications.

All the available data on vibrational frequencies for thiophene and its deuterated analogues, as well as the two conformers of TA including frequency shifts for the C=O stretching mode [38, 40] and centrifugal distortion constants have been used for refining the force field.

From the initial force field, the vibrational frequencies and distortion constants of TA were calculated on the average within 2% of the observed values. The doublet near 670 cm^{-1}, ν_{17} and ν_{18}, was calculated with a splitting of 40 cm^{-1}, in contrast to the observed 7 cm^{-1}. Further, the inertial defect for the vibrational ground state and the isotopic frequency shifts for the C=O stretching mode were calculated with wrong magnitudes.

However, only minor changes in the force constants were necessary in order to obtain an excellent agreement with all observed data. A study of the Jacobian elements revealed that the isotopic shifts for the C=O stretching mode depended significantly, among others, upon the C=O/C—C=O, the C=O/C—H_{ald} and the C=O/C—C_{ald} interaction constants. However, the available data is insufficient for determining all these constants. In formaldehyde the C=O/C—H force constant has been determined as 0.52 mdyn $Å^{-1}$, and for all the compounds X_2CO (C = H, F, Cl), the C=O/O=C—X interaction is remarkably constant, ca. 0.5 mdyn rad^{-1} [49—51]. We have

TABLE 5

Observed and calculated spectroscopic data and potential energy distribution (PED)[a]

		Syn			*Anti*		
		Obs.	Calc.	PED	Obs.	Calc.	PED
A'	ν_1	3121	3129	$97s_3$		3129	$97s_3$
	ν_2	3099	3095	$51s_2 + 46s_1$		3095	$51s_2 + 45s_1$
	ν_3	3086	3093	$52s_1 + 46s_2$		3093	$53s_1 + 45s_2$
	ν_4	2821	2821	$99r$		2820	$99r$
	ν_5	1705	1705	$99c$	1705	1702	$96c$
	ν_6	1524	1522	$52d_1 + 34d_2$	1519	1524	$54d_1 + 33d_2$
	ν_7	1425	1432	$63d_2 + 30d_1 + 13q$	1432	1431	$69d_2 + 35d_1$
	ν_8	1380	1380	$40\beta + 33\alpha$	1393	1392	$44\beta + 33\alpha + 10q$
	ν_9	1340	1343	$33h + 16\delta'_2 + 16\delta_3 + 10\delta'_3$	1358	1338	$42h + 17\delta'_2 + 17\delta_3 + 10\delta'_3$
	ν_{10}	1232	1228	$27d_1 + 25h + 17p_1$	1241	1229	$21\delta'_1 + 20\delta_1 + 16h + 14q + 11d_2$
	ν_{11}	1211	1207	$21h + 21\delta_1 + 20\delta'_1 + 17q + 10d_2$	1146	1154	$24d_1 + 20q + 15p_1 + 10\delta'_1$
	ν_{12}	1084	1084	$23\delta'_2 + 22\delta_3 + 21\delta_2 + 21\delta'_3$	1079	1074	$22\delta_3 + 22\delta'_3 + 19\delta'_2 + 14\delta_2 + 10d_1$
	ν_{13}	1044	1047	$51h + 15\delta_1$	1034	1043	$47h + 16\delta_1$
	ν_{14}	864	868	$47p_2 + 23\omega_2 + 17\omega_3$	862	861	$58p_2 + 19\omega_2 + 17\omega_3$
	ν_{15}	760	776	$60p_2 + 12\omega_1 + 16\sigma$	815	814	$49p_1 + 37\sigma$
	ν_{16}	672	676	$111p_1$	749	751	$57p_2 + 15p_1$
	ν_{17}	665	660	$28\sigma + 11p_1 + 10p_2$	583	591	$41p_1 + 27\rho + 13\omega_3 + 11\sigma$
	ν_{18}	454	452	$20q + 17\rho + 15\omega_4$	420	420	$18q + 16\sigma + 14\omega_4 + 12p_1$
	ν_{19}	173	164	$58\gamma' + 54\gamma + 10\sigma + 10p_1$	195[c]	186	$57\gamma + 53\gamma' + 12p_1$
A''	ν_{20}	990	990	$91\pi_3$		994	$91\pi_3$
	ν_{21}	911	912	$75\pi_2 + 34\pi_1 + 17\pi_3 + 15\tau_2$		912	$74\pi_2 + 35\pi_1 + 17\pi_3 + 15\tau_2$
	ν_{22}	834	839	$82\pi_1 + 19\pi_3 + 12\pi_2$	844	839	$82\pi_1 + 19\pi_3 + 12\pi_2$
	ν_{23}	720	720	$81\pi_3 + 38\pi_2$	718	720	$81\pi_3 + 38\pi_2$
	ν_{24}	566	566	$110\tau_1 + 66\tau_2 + 30\pi_4$		566	$108\tau_1 + 68\tau_2 + 29\pi_4$
	ν_{25}	471	469	$94\tau_2 + 43\pi_4 + 20\tau_1$	464	463	$94\tau_2 + 43\pi_4 + 23\tau_1$
	ν_{26}	257	256	$28\tau_3 + 26\pi_4 + 21\tau_1$	238	237	$41\pi_4 + 21\tau_3 + 20\tau_1$
	ν_{27}	122	122	$75\tau_3 + 22\pi_4$		137	$75\tau_3$
	ν_5—ν_5 (CDO)	15[d]	15				
	ν_5—ν_5 (^{18}O)	33[e]	33				

	Syn	
	Obs.	Calc.
Δ_J	0.1477	0.1404
Δ_{JK}	0.854	0.784
Δ_K	0.246	0.243
δ_J	0.0396	0.0390
δ_K	0.678	0.672
ID ($v = 0$)	0.00893	0.01572
ID ($v_{19} = 1$)	1.043	1.040
ID ($v_{26} = 1$)	—0.220	—0.225
ID ($v_{27} = 1$)	—1.2122	—1.1835

[a]See Fig. 9 for an explanation of the internal coordinates. τ_1 and τ_2 are ring torsions and τ_3 is the torsion of the aldehyde group relative to the thiophene ring. [b]Frequencies in cm^{-1}, distortion constants (Δ, δ) in kHz and inertial defects (ID) in uA^2. [c]Not included in the refinement. [d]From ref. 40. [e]From ref. 38.

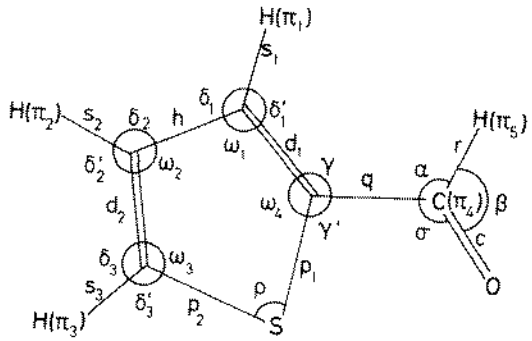

Fig. 9. Explanation of the internal coordinates used in Table 5. Latin letters denote stretching movements and greek letters denote bending vibrations. Out-of-plane bendings are denoted by π.

therefore transferred these values with confidence in the final refinement. The initial and final set of valence force constants are presented in Table 4, while observed and calculated data for TA are given in Table 5 together with the potential energy distribution (see Fig. 9 for an explanation of the internal coordinates). The overall agreement is within 0.7% on the average. As seen, the inertial defects are calculated very close to the observed values, the deviation in no case being larger than what can be accounted for by the electronic contribution.

Structure analysis from the electron diffraction results

An experimental radial distribution (RD) curve (Fig. 10) was calculated in the usual way by the Fourier transformation of the function: $I'_m(s) = sI_m(s) \cdot Z_C Z_{Cl} A_C^{-1} A_{Cl}^{-1} \exp(-Bs^2)$ with $B = 0.0020$ Å^2. The experimental intensity curve used in this calculation was obtained by averaging the two intensity curves of Fig. 2 and using theoretical data for $s < 2.00$ Å^{-1}. Theoretical RD curves were calculated for conformers with O and S *syn* (torsion angle $\phi = 0$) or *anti* ($\phi = 180°$), using reasonable values for bond distances and valence angles. The torsion-sensitive part of the experimental RD curve is shown in Fig. 11 together with theoretical curves for the two conformers and for a mixture of 80% *syn* and 20% *anti*. From these curves it was obvious that the major conformer was OS *syn*. However, the shoulder on the experimental peak at about 3.9 Å clearly showed that some of the *anti* conformer had to be present in the gas phase at 367 K.

Least-squares refinements [52] of the structure were carried out by fitting a single theoretical intensity curve to the two average experimental curves of Fig. 2, and simultaneously, the three corresponding calculated rotational constants to the experimental ones from the microwave part of the present study. Because of the effect of vibrational averaging the r_a distances used in calculating the theoretical intensity curve are inappropriate for rotational

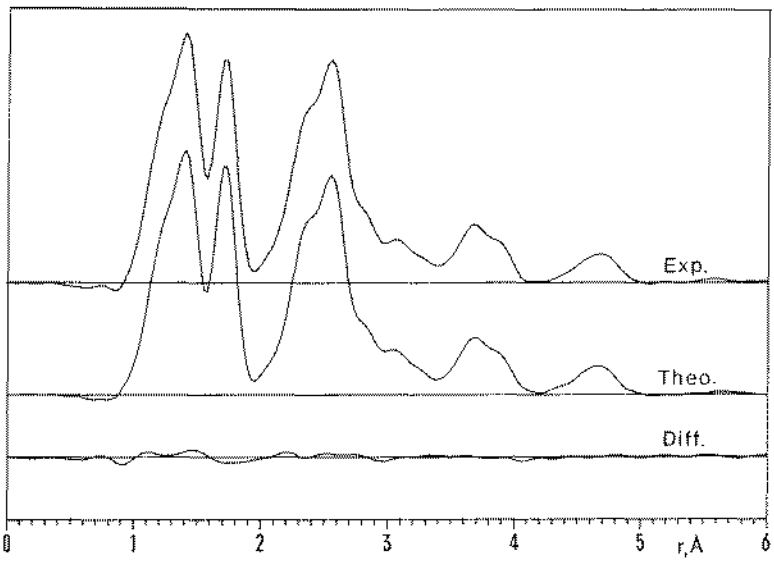

Fig. 10. Radial distribution curves calculated from the intensity curves of Fig. 2 after multiplication by $Z_C Z_S / A_C A_S \exp(-Bs^2)$ with $B = 0.002$ Å^2. Theoretical intensity data were used in the experimental curve for $s < 2.0$ Å^{-1}.

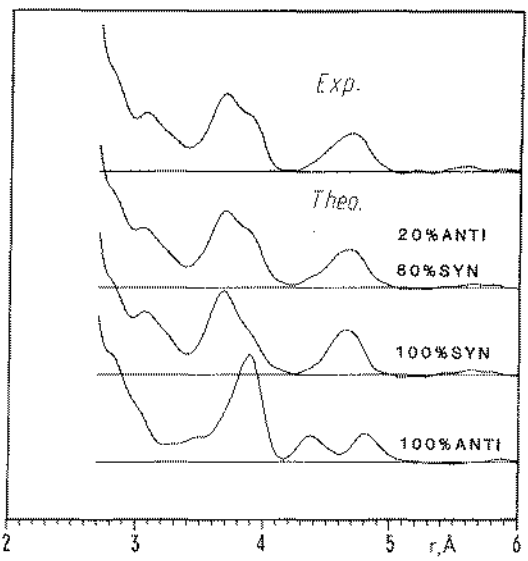

Fig. 11. Theoretical radial distribution curves for conformers with O and S either *syn* or *anti* and for a mixture of the two conformers together with the experimental curve. Only the conformationally important parts of the curves are shown.

constants. We defined our models in terms of the geometrically consistent $r_\alpha^0 = r_z$ set of distances which were used to calculate rotational constants B_z related to the observed B_0 by $B_z = B_0 + 0.5\ \Sigma_s \alpha_s^{har}$. The r_a distances for the temperature T of interest were calculated from the r_α^0 set of the model according to ref. 53

$$r_a^T = r_\alpha^0 + 1.5\ a_3[(l^2)^T - (l^2)^0] + \delta_r^T + K^0 - (l^2)/r_\alpha^0$$

The Morse function anharmonicity constants a_3 were given the diatomic molecule values for bonds [54] and otherwise assumed to be zero. Values for centrifugal distortion (δ_r), perpendicular amplitudes (K) and mean-square amplitudes of vibration (l^2), as well as α^{har} were calculated from the valence force field described earlier. Assuming the two conformers of TA to have equal geometry apart from the S—C—C=O torsion angle ϕ, and assuming the thiophene ring to have C_{2v} symmetry, TA can be described by 12 geometrical parameters, in our refinements taken as: r(C—H), r(C=O), $\langle r(C—C)\rangle = 0.5(r(C_1{=}C_2) + r(C_2{—}C_3))$, $\Delta r(C—C) = r(C_2{—}C_3) - r(C_1{=}C_2)$, $r(C_1{—}C_5)$, r(C—S), $\angle C_5{—}C_1{=}C_2$, $\angle C_2{=}C_1{—}S$, $\angle C{=}C{—}H$, $\angle C{—}C{=}O$, $\angle C_1{—}C_5{—}H$ and ϕ, the S—C—C=O torsion angle for the *anti* conformer. All C—H distances were assumed to be equal. The root-mean-square amplitudes of vibration (l) were all, except l(C—S), kept constant in the least squares refinements at the values calculated from the described valence force field.

For the *syn* form a dynamic model was used where this conformer was represented by five distinct forms with different torsion angles, each weighted according to a gaussian potential function. The r.m.s. amplitude for the torsional vibration (τ) was introduced as a parameter, and it was refined in the least-squares refinements [26]. The angle $\angle C_1{—}C_5{—}H$ could not be determined very well in the refinements, and it was therefore given a reasonable value and kept constant. The results of the final least-squares refinements are listed in Table 6. The theoretical intensity and RD-curves calculated from these results together with experimental and difference curves are shown in Figs. 2 and 9, respectively. Table 7 gives the correlation matrix for the refined parameters.

DISCUSSION

Our combined electron diffraction and spectroscopic investigation of TA has shown that the major conformer is the one with O and S *syn*. This is in agreement with earlier experimental results [5—13]. In addition, we have observed (ED and IR) substantial amounts (ca. 20%) of a second conformer where O and S are *anti* to each other. Compared to earlier spectroscopic investigations we have observed a number of *anti* absorptions. In Table 6 we have reported a torsion angle of 158.5 ± 23.1° for this form. This was the result obtained from the electron diffraction data when a torsionally stiff model was used. However, the ED data are also consistent with a planar conformer undergoing large torsional motions (like the *syn* form) or with a

TABLE 6

Final parameter values[a] for the structure of thiophene-2-aldehyde

Parameter	$r_a/\angle_\alpha$	l	Parameter	$r_a/\angle_\alpha$	l
r(C—H)	1.114(20)	0.078	*Selected dependent angles and distances*		
r(C=O)	1.224(7)	0.038	$\angle C_1{=}C_2{-}C_3$	112.2(3)	
r(C—S)	1.717(4)	0.046(4)	$\angle$C—S—C	92.0(4)	
$r(C_1{-}C_5)$	1.466(16)	0.049	$\angle$S—C_1—C_5	121.9(1.0)	
$\angle r$(C—C)[b]	1.403(7)		r(C=C)	1.375(7)	0.045
Δr(C—C)[c]	0.056(16)		$r(C_2{-}C_3)$	1.431(15)	0.049
$\angle C_2{=}C_1{-}C_5$	126.4(1.3)		$r(C_1\cdots C_3)$	2.328(8)	0.053
$\angle$C=C—S	111.8(4)		$r(C_2\cdots C_5)$	2.532(24)	0.069
$\angle$C=C—H	129.2(4.0)		$r(C_2\cdots$S)	2.575(6)	0.052
$\angle$C=C—O	123.7(9)		$r(C_5\cdots$S)	2.781(11)	0.075
$\angle C_1{-}C_5{-}$H	[115.0]		$r(C_1\cdots C_4)$	2.469(11)	0.059
τ[d]	17.2(13.6)		$r(C_1\cdots$O)	2.371(11)	0.059
$\angle\phi$[e]	158.5(23.1)		$r(C_3\cdots C_5)$	3.741(12)	0.065
% *syn*	80.5(7.9)		$r(C_4\cdots C_5)$	3.904(11)	0.069
			$r(C_2\cdots$O) (*syn*)	3.636(14)	0.062
			$r(C_3\cdots$O) (*syn*)	4.688(10)	0.074
			$r(C_4\cdots$O) (*syn*)	4.552(11)	0.110
			r(S···O) (*syn*)	3.075(15)	0.133
			$r(C_2\cdots$O) (*anti*)	2.981(51)	0.102
			$r(C_3\cdots$O) (*anti*)	4.360(19)	0.091
			$r(C_4\cdots$O) (*anti*)	4.805(21)	0.070
			r(S···O) (*anti*)	3.895(36)	0.069

[a]Distances (r_a) and vibrational amplitudes (l) in Å, angles in degrees. Parenthesized uncertainties are 2σ and include estimates of systematic errors and correlation in the experimental data. [b]$\langle r(\text{C—C})\rangle = 0.5(r(C_1{=}C_2) + r(C_2{-}C_3))$. [c]$\Delta r(\text{C—C}) = r(C_2{-}C_3) - r(C_1{=}C_2)$. [d]$\tau$ is the root mean square torsional amplitude for the *syn* form. [e]$\angle\phi$ is the S—C—C=O torsion angle for the *anti* form.

TABLE 7

Correlation matrix × 100 for the parameters of thiophene-2-aldehyde

Parameter	σ[a]	r_1	r_2	r_3	r_4	r_5	r_6	$\angle_7$	$\angle_8$	$\angle_9$	$\angle_{10}$	τ	$\angle_{12}$	l	% *syn*
1 $\langle r$(C—C)$\rangle$	0.0016	100	75	0	22	−71	22	−48	25	−40	0	−19	−10	18	4
2 Δr(C—C)	0.0047		100	8	−3	−61	−22	−63	68	−27	37	−37	−5	25	−4
3 r(C—S)	0.0006			100	−5	−11	−20	12	−21	4	4	−3	−5	−12	−1
4 r(C—H)	0.0050				100	−27	32	16	−31	−29	−18	20	6	−29	11
5 r(C—COH)	0.0038					100	−15	62	−27	47	−36	32	13	−4	11
6 r(C=O)	0.0017						100	10	−37	−24	−48	22	−8	−2	8
7 $\angle$C=C—COH	0.42							100	−71	73	−14	46	36	−25	8
8 $\angle$C=C—S	0.14								100	−29	46	−43	−9	35	−10
9 $\angle$C=C—H	1.33									100	29	22	39	−10	−4
10 $\angle$C—C=O	0.30										100	−29	24	7	−21
11 τ	4.54											100	2	−13	1
12 $\angle\phi$	7.71												100	−1	4
13 l(C—S)	0.0010													100	−6
14 % *syn*	2.64														100

[a]Standard deviations from least squares.

model having a low torsional barrier at the planar position. The electron diffraction experiment cannot distinguish between these possibilities. When a dynamic model like the one described for the *syn* was used also for *anti* a r.m.s. torsional amplitude of 26 ± 24° was obtained, and the *R*-factor had the same value as with a torsional stiff model.

Microwave spectroscopy has shown that the *syn* conformer is planar, and, from the electron diffraction data, using a dynamic model, we found a r.m.s. torsional amplitude of $\tau = 17°$ for *syn*. With the assumption that the torsional motion is harmonic, a value of the *syn* torsional force constant may be obtained from τ by: $f_\tau = 0.5 \cdot V^* = RT/\tau^2$. The result is $f_\tau = 0.058$ mdyn Å rad^{-2}, in excellent agreement with the value of 0.054 mdyn Å rad^{-2} obtained from the observed torsional frequency. It should be noted, however, that the error limits on τ are large. For $V^* = V_1 + 4V_2 + 9V_3 + \ldots$ the value of τ corresponds to $V^* = 69.5$ kJ mol^{-1}.

If we assume the two conformers of TA to have approximately the same entropy, the conformational composition observed in electron diffraction corresponds to an energy difference of 4.3 ± 1.6 kJ mol^{-1}, which is in excellent agreement with the value of ΔH^0 obtained from the matrix experiments (4.1 ± 0.4 kJ mol^{-1}). Our result is also in good agreement with the result from ab initio molecular orbital calculations [14] (3.0—3.6 kJ mol^{-1}), from ultrasonic relaxation measurements [7] ($\Delta H^0 < 6.7$ kJ mol^{-1}) and from measurements of dipole moments and Kerr constants [8] (83 ± 10% *syn* in cyclohexane solution at 25°C). The result is very different from that obtained for furan-2-aldehyde where the energy difference was observed to be $\Delta H^0 =$ —4.2 ± 0.8 kJ mol^{-1} [3], which means that *anti* is the more stable form. The enhanced stability of the *syn* form of TA relative to furan-2-aldehyde has been attributed to a stabilizing interaction between the sulphur and oxygen atoms, a view which is supported by theoretical studies [10, 12, 55].

TABLE 8

Geometry of thiophene-2-aldehyde and some related molecules[a]

Parameter	Thiophene-2-aldehyde	Thiophene	Furan-2-aldehyde
r(C=O)	1.224(7)		1.212(4)
r(C—COH)	1.466(16)		1.453(7)
r(C=C)	1.375(7)	1.368(6)	[1.361]
r(C—C)ring	1.431(15)	1.429(20)	[1.431]
r(C—X)	1.717(4)	1.717(4)	[1.362]
∠C=C—COH	126.4(1.3)		131.7(4)
∠C—C=O	123.7(9)		122.7(8)
∠C=C—C	112.2(3)	112.3(6)	[106.1]
∠C=C—X	111.8(4)	111.7(6)	[110.7]
∠C—X—C	92.0(4)	92.0(5)	[106.5]
Ref.	This work	54	3

[a]Distances (r_a) in Å, angles in degrees. Quantities in square brackets were assumed.

In Table 8 the geometrical parameters of TA are compared with those of thiophene and furan-2-aldehyde. As can be seen, the effect of the aldehyde group on the rest of the molecule is very small, the geometry of the ring being almost identical in thiophene [56] and TA. The distance r(C—O) in furan-2-aldehyde is of course quite different from r(C—S) in TA, and the valence angles in the two rings are therefore somewhat different. But, apart from this, the only major difference in the geometry of the two aldehydes is in ∠C=C—COH where a significantly larger value (131.7(4)°) is observed in furan-2-aldehyde compared to the value of 126.4(1.3)° found in TA. We have no good explanation for this discrepancy.

ACKNOWLEDGEMENTS

The authors are grateful to Prof. S. Gronowitz, The University of Lund, for providing us with the sample of TA and to siv. ing. Ragnhild Seip and Ms. S. Gundersen, The University of Oslo, for recording the electron diffraction data and running the first computer programs. C. J. N. thanks the staff of Chemical Laboratory V, University of Copenhagen, for the use of their equipment and their kind hospitality. Financial support from the Norwegian Research Council for Science and the Humanities (NAVF) as well as the Nansen Foundation is acknowledged.

REFERENCES

1 R. J. Abraham and T. M. Siverns, Tetrahedron, 28 (1972) 3015.
2 D. J. Chadwick, J. Chem. Soc., Perkin Trans. 2, (1976) 451.
3 G. Schultz, I. Fellegvári, M. Kolonits, A. I. Kiss, B. Pete and J. Bánke, J. Mol. Struct., 50 (1978) 325.
4 K. Hagen, J. Mol. Struct., 130 (1985) 255.
5 F. Mönnig, H. Dreizler and H. D. Rudolph, Z. Naturforsch, Teil. A, 20 (1965) 1323.
6 J. F. Bertrán, E. Ortiz and L. Ballester, J. Mol. Struct., 17 (1973) 161.
7 R. A. Pethrick and E. Wyn-Jones, J. Chem. Soc. A, (1969) 713.
8 C. L. Cheng, I. G. John, G. L. D. Ritchie, P. H. Gore and L. Farnell, J. Chem. Soc., Perkin Trans. 2, (1975) 744.
9 M. L. Martin, C. Andrieu and G. J. Martin, Bull. Soc. Chim. Fr., (1968) 698.
10 B. Roques and M. C. Fournie-Zaluski, Org. Magn. Reson., 3 (1971) 305.
11 S. Combrisson, B. Roques, P. Rigny and J. J. Bassilier, Can. J. Chem., 49 (1971) 905.
12 S. Nagata, Y. Yamabe, K. Yoshikawa and H. Kato, Tetrahedron, 29 (1973) 2545.
13 D. J. Chadwick, G. D. Meakins and E. E. Richards, Tetrahedron Lett., 36 (1974) 3183.
14 J. Kao and L. Radom, J. Am. Chem. Soc., 101 (1979) 311.
15 Hs. H. Günthard, J. Mol. Struct., 80 (1982) 87, and references cited therein.
16 P. Felder and Hs. H. Günthard, Spectrochim. Acta, Part A, 36 (1980) 223.
17 S. Mizushima, T. Shimanouchi, I. Harada, Y. Abe and H. Takeuchi, Can. J. Phys., 53 (1975) 2085.
18 K. Tanabe, Spectrochim. Acta, Part A, 28 (1972) 407.
19 K. Kveseth, Acta Chem. Scand., Ser. A, 28 (1974) 482.
20 K. Kveseth, Acta Chem. Scand., Ser. A, 29 (1975) 307.
21 T. Stroyer-Hansen, Infrared Phys., 10 (1970) 159.
22 B. Gilbert and G. Duyckaerts, Spectrochim. Acta, Part A, 26 (1970) 2197.

23 W. Zeil, J. Haase and L. Wegmann, Z. Instrumentenkd., 74 (1966) 84.
24 O. Bastiansen, R. Graber and L. Wegmann, Balzers High Vac. Rep., 25 (1969) 1.
25 K. Tamagawa, T. Iijima and M. Kimura, J. Mol. Struct., 30 (1976) 243.
26 K. Hagen and K. Hedberg, J. Am. Chem. Soc., 95 (1973) 1003.
27 G. Gundersen and K. Hedberg, J. Chem. Phys., 51 (1969) 2500.
28 L. Hedberg, Abstr., 5th Austin Symp. Gas Phase Molecular Structure; Austin, TX, March 1974, p. 37.
29 Available from B.L.L.D. as Suppl. Publ. No. SUP 26304 (4 pages).
30 J. K. G. Watson, J. Chem. Phys., 46 (1967) 1935.
31 B. Bak, D. Christensen, L. Hansen-Nygaard and J. Rastrup-Andersen, J. Mol. Spectrosc., 7 (1961) 58.
32 A. E. Cherniak and C. C. Costain, J. Chem. Phys., 45 (1966) 104.
33 P. Chiorboli and A. M. Drusiani, Rendiconti, XII (1952) 309.
34 A. R. Katritzky and A. J. Boulton, J. Chem. Soc., (1959) 657.
35 Joeckle, E. Lemperle and R. Mecke, Z. Naturforsch., Teil A, 22 (1967) 403.
36 J.-J. Péron, P. Saumagne and J.-M. Lebas, C. R. Acad. Sci., Ser. B, 264 (1967) 797.
37 J.-J. Péron, P. Saumagne and J.-M. Lebas, Spectrochim. Acta, Part A, 26 (1970) 1651.
38 C. Andrieu, R. Pinel and Y. Mollier, Bull. Soc. Chim. Fr., (1971) 1314.
39 D. J. Chadwick, J. Chambers, G. D. Meakins and R. L. Snowden, J. Chem. Soc., Chem. Commun., (1972) 742.
40 D. J. Chadwick, J. Chambers, G. D. Meakins and R. L. Snowden, J. Chem. Soc., Perkin Trans. 2, (1975) 604.
41 C. E. Blom, R. P. Müller and Hs. H. Günthard, Chem. Phys. Lett., 73 (1980) 483.
42 P. Felder and Hs. H. Günthard, Chem. Phys. Lett., 66 (1979) 283.
43 P. Huber-Wälchli, Ber. Bunsenges. Phys. Chem., 82 (1978) 10.
44 P. Huber-Wälchli and Hs. H. Günthard, Chem. Phys. Lett., 30 (1975) 347.
45 G. O. Braathen, Spectrochim. Acta, Part A, 41 (1985) 933.
46 W. A. Seth-Paul, J. Mol. Struct., 3 (1969) 403.
47 D. W. Scott, J. Mol. Spectrosc., 31 (1969) 451.
48 P. Cosse and J. H. Schachtschneider, J. Chem. Phys., 44 (1966) 97.
49 J. L. Duncan and P. D. Mallison, Chem. Phys. Lett., 23 (1973) 597.
50 P. D. Mallison, D. C. McKean, J. H. Holloway and I. A. Oxton, Spectrochim. Acta, Part A, 31 (1975) 143.
51 H. G. Schnöckel, J. Mol. Struct., 29 (1975) 123.
52 K. Hedberg and M. Iwasaki, Acta Crystallogr., 17 (1964) 529.
53 K. Kuchitsu and S. J. Cyvin, in S. J. Cyvin (Ed.), Molecular Structures and Vibrations, Elsevier, Amsterdam, 1972, Chap. 12.
54 K. Kuchitsu and Y. Morino, Bull. Chem. Soc. Jpn., 38 (1965) 805.
55 L. Lunazzi and C. A. Veracini, J. Chem. Soc., Perkin Trans. 2, (1973) 1739.
56 J. H. Callomon, E. Hirota, K. Kuchitsu, W. J. Lafferty, A. G. Maki and C. S. Pote, Structure Data of Free Polyatomic Molecules, Landolt-Börnstein, New Series, Vol. 7, Springer-Verlag, Berlin, 1976.